*Astronomy & Astrophysics* manuscript no. main
September 1, 2014


# Nickel mass estimates of Type Ia Supernovae from NIR data: Test case for SN2014J and SN2006X

**TBD**

[1] European Southern Observatory, Karl Schwarzschild Strasse 2, Garching bei Munchen, Germany, 85748
e-mail: @eso.org
[2]

Preprint online version: September 1, 2014

**Abstract**

*Aims.* To determine the relation between the amount of Nickel produced in SNIa and the timing of the second maximum and to extrapolate Nickel mass values for highly reddened SNIa using this relation
*Methods.* We measure the (pseudo)-bolometric luminosity at peak and use it to derive a value of $M_{Ni}$ mass for a 'low-reddening' sample of objects from the literature in order to minimize effects from presuming a reddening law.
*Results.* We find a strong correlation between the $M_{Ni}$ and $t_2$ in the $Y$ and $J$ bands and a weaker trend in the $H$ band. We use this empirical relation to derive $M_{Ni}$ for two test case SN with high extinction ($> 1.2$ mag). This allows us to have a $M_{Ni}$ value which is independent of the reddening law applied.
*Conclusions.* From our results we conclude that an empirical relation between $M_{Ni}$ and $t_2$ can allow us to infer the $M_{Ni}$ for highly reddened objects without an estimate of their total absorption. The results for SN2014J from this method correspond well with the values obtained from recent $\gamma$ ray observations, thus providing further evidence of the potency of this technique

**Key words.** stars: supernovae: general

## 1. Introduction

The uniformity of Type Ia supernovae (SNe Ia) has led to their use as cosmological distance indicators (reviewed in: **???**). As cosmological probes the SNe Ia provided the first evidence for the accelerated expansion of the universe (**??**).

Observations of large samples of SNe Ia show that the peak luminosity in the optical is not uniform (e.g. **??????**), leading to different bolometric luminosities for the objects (**?**) implying variations in the physical parameters of the explosion, in particular the synthesised nickel mass and the total ejected mass (**??**). The correlation at optical wavelengths between peak luminosity and light curve shape together with the determination of the absorption towards the supernova are the key ingredients of the calibration of these objects prior to their use as distance indicators (**?**).

At near infrared wavelengths SNeIa display a very uniform brightness behaviour (**????**). The scatter in the peak luminosity in these studies is 0.2 magnitudes, which, combined with the lower sensitivity of the IR to extinction by dust, has sparked increased interest in this wavelength region. Statistically significant samples of SN Ia light curves are thus becoming available (**????**) and have been used to construct the first rest-frame near-infrared Hubble diagrams (**????**).

The light curve morphology in the infrared is markedly different from that in the optical, with a pronounced secondary maximum in $IYJHK$ filters for 'normal' SNe Ia and a 'shoulder' in the $V$ and $R$ filter light curves (**??????**). **?** demonstrated that the second maximum could be the result of decrease in opacity due to the ionization change of Fe group elements from doubly to singly ionized atoms, which preferentially radiate the energy at near-IR wavelengths. He further indicated that larger iron mass would lead to a later maximum in the IR light curves.

Recent studies have shown a strong dependence of the timing of the second maximum (hereafter $t_2$) on the decline rate of the SNIa, indicating that brighter explosions have a later onset of the second maximum. A strong relation between the $t_2$ and the onset of the uniform optical colour phase (hereafter $t_L$, see also $t_{max}$ **?**) suggests that the second maximum is related to the colour evolution which is tied to the amount of iron group elements synthesized in the explosion (**?**). The conclusion from these studies point to a connection between the $M_{^{56}Ni}$ in SNIa and $t_2$.

In this study, we investigate ,directly, the link between the $M_{^{56}Ni}$ and $t_2$. We use a sample of nearby objects with low extinction from dust, in order to circumvent uncertainties from the specific reddening law used. We aim to use this relation to derive $M_{^{56}Ni}$ for heavily extinguished SNae where using the bolometric peak is extremely sensitive to the total absorption value used, and hence, the reddening law. To this end, we propose using NIR only data at late times along with an empirical relation to obtain precise estimates of $M_{^{56}Ni}$ for objects where other methods provide disparate results.

## 2. Data

The sample for this study is constrained by objects which have NIR observations at late times as well as well-sampled optical light curves to construct a (pseudo-) bolometric light curve. The main data source of near-infrared photometry of SNe Ia currently comes from the Carnegie Supernova Project (CSP; **?????**). They

*Send offprint requests to*: TBD

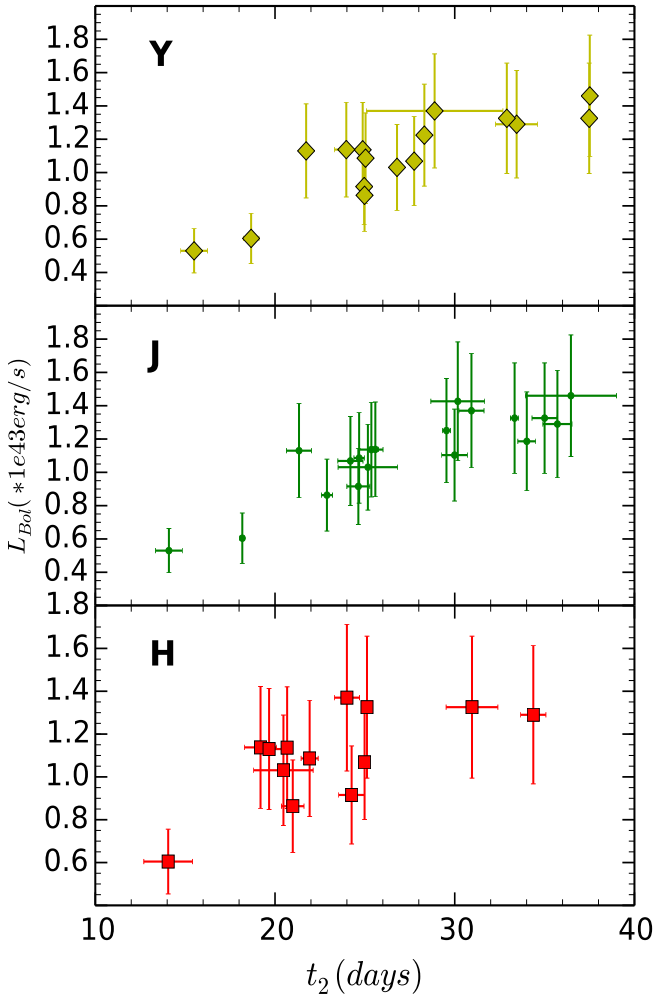


Figure 1 $L_{max}$ is plotted against the $t_2$ in $YJH$ bands. A strong correlation is observed in the $Y$ and $J$, whereas a weaker correlation is seen in the $H$ band. **this only includes objects with a u-H measured bolometric peak and not any of the others**

form an ideal basis for an evaluation of light curves parameters. We add to this sample objects from the literature and the nearby objects SN2011fe.

Since we aim to circumvent the uncertainties from host galaxy extinction, we only select objects with an $E(B-V)_host$ value less than 0.1. Since we want to investigate the connection of $M_{Ni}$ with $t_2$ in the NIR, this excludes objects which are spectroscopically similar to the peculiar SN 1991bg (**???**) and objects that do not exhibit a second maximum (SNe 2005bl, 2005ke, 2005ku, 2006bd, 2006mr, 2007N, 2007ax, SN2007ba, 2009F). On similar lines we exclude peculiar objects like 2006bt and 2006ot. These constraints leave us with a final sample of 22 objects.

## 3. Analysis

The flux emitted by an SNIa in the UV, optical and NIR traces the radiation converted from the radioactive decays of newly synthesized isotopes. As the SN emits most of its flux in the UV to NIR passbands, the "uvoir bolometric flux" represents a physically meaningful quantity (**?**)

We select a low-reddening sample so that our measurements are less sensitive to a reddening law. For objects with sufficient amount of near maximum data in the optical and the NIR, we construct UBVRIJH bolometric light curves. We do not use $K$ band data since there are very few objects in the sample with well-sampled $K$ band light curves. For objects with well-sampled $K$ light curves we calculate the flux emitted in the $K$ band and find that it is between $1-3\%$, thus, not using the $K$-band is not a dominant source of uncertainty. The magnitudes were corrected for reddening using a CCM reddening law for each filter. The values for the extinction are presented in table 2. The uncertainty in the reddening estimate was propagated into the calculation of the bolometric flux Using zero-points in the given filters, the magnitudes were converted to fluxes. The resulting light curve, in ergs/$cm^2$/s was converted into an absolute bolometric light curve by using the distances of the SN derived from the host galaxy redshift.

Since all distances are scaled to an $H_0 = 70kms^{-1}Mpc^{-1}$the errors in the luminosity distance are only affected by the relative errors in the distance moduli (see Table 2 for values and uncertainty estimates). For objects not in the hubble flow, we use distance measurements from published estimates (which use others methods eg. Cepheid, Tully-Fisher relation etc.).

The bolometric light curves were interpolated using a cubic spline. In order to get an $L_{Bol}(max)$ we required sampling in the individual bands at pre-maximum epochs. Thus, for objects without NIR coverage before $B_{max}$, we use the UBVRI light curves. The errors on the peak were calculated from the errors in the fluxes of the bolometric maximum using a Monte Carlo for 1000 realisations of the light curve.

For objects with no NIR coverage near maximum, we apply a correction like in **?** and increase the $M_{Ni}$ value by 1.1. In **?**, the authors found that using a UVOIR light curve with the correction for the NIR, Arnett's rule estimates the $M_{Ni}$ to $\leq 0.05\ M_\odot$.

## 4. Results

In this section we present the results derived from the measurements of the peak bolometric luminosity and the trends observed with other observables for the SNe in our low-reddening sample, as well as the complete sample of objects with a measured timing of the second maximum

### 4.1. Correlation between $L_{max}$ and $t_2$

In figure 1, we find that there is a very strong correlation between $t_2$ and $M_{Ni}$ in the $Y$ and $J$ bands with $r$ values of 0.80, 0.88. A much weaker trend is observed in the $H$ band with $r \sim 0.60$. This is reflected in the ratio of the slope to the slope error in equation (1)

In the $Y$ and $J$ band, a strong correlation suggests that objects with more Ni produced show later second maxima.

$$L_{max} = a_i \cdot t_2(i) - b_i \tag{1}$$

The scatter around the best fit in $YJH$ bands is 0.18, 0.16 and 0.22 ($* e^{43}ergs^{-1}$) respectively. This reflects the strength of the correlations in the individual bands

Table 1 The sample of SNe which have low reddening, as defined in the text. The references for the data are presented along with the extinction values and the distanes used to calculate the bolometric light curves **to add: distance modulus values**

| SN | $\mu$ | $e_\mu$ | $E(B-V)_{host}$ | $E(B-V)_{MW}$ | Filters |
|---|---|---|---|---|---|
| SN2008gp | 0.66 | 0.14 | 0.098(0.022) | 0.104(0.005) | UBVRIJH |
| SN2007as | 0.44 | 0.05 | 0.050(0.011) | 0.123(0.001) | UBVRI |
| SN2008bc | 0.68 | 0.19 | $< 0.019$ | 0.225(0.004) | UBVRIJH |
| SN2008hv | 0.49 | 0.13 | 0.074(0.023) | 0.028(0.001) | UBVRIJH |
| SN2008ia | 0.6 | 0.14 | 0.066(0.016) | 0.195(0.005) | UBVRIJH |
| SN2005na | 0.79 | 0.24 | 0.061(0.022) | 0.068(0.003) | UBVRI |
| SN2005eq | 0.73 | 0.2 | 0.044(0.024) | 0.063(0.003) | UBVRIJH |
| SN2005M | 0.76 | 0.08 | 0.060(0.021) | 0.027(0.002) | UBVRIJH |
| SN2007on | 0.3 | 0.09 | $< 0.007$ | 0.010(0.001) | UBVRIJH |
| SN2007nq | 0.58 | 0.17 | 0.046(0.013) | 0.031(0.001) | BVRI |
| SN2005am | 0.48 | 0.2 | 0.053(0.017) | 0.043(0.002) | UBVRIJH |
| SN2005hc | 0.8 | 0.2 | 0.049(0.019) | 0.028(0.001) | UBVRIJH |
| SN2004gu | 0.74 | 0.15 | 0.096(0.034) | 0.022(0.001) | BVRI |
| SN2011fe | 0.52 | 0.15 | 0.03(0.01) | 0.021(0.001) | UBVRIJH |
| SN2001ba | 0.58 | 0.15 | 0.06(0.02) | 0.08 (0.002) | UBVRIJH |
| SN2002dj | 0.64 | 0.26 | 0.04(0.03) | 0.06 (0.003) | UBVRIJH |
| SN2002fk | 0.74 | 0.23 | 0.07(0.02) | 0.02 (0.003) | UBVRIJH |
| SN2008R | 0.25 | 0.1 | 0.009(0.013) | 0.062(0.001) | UBVRIJH |
| SN2005iq | 0.52 | 0.11 | 0.040(0.015) | 0.019(0.001) | UBVRIJH |
| SN2005ki | 0.51 | 0.27 | 0.016(0.013) | 0.027(0.001) | UBVRIJH |
| SN2006bh | 0.42 | 0.15 | 0.037(0.013) | 0.023(0.001) | UBVRIJH |
| SN2007bd | 0.6 | 0.13 | 0.058(0.022) | 0.029(0.001) | UBVRIJH |

Table 2 $L_{max}$ measurements for low reddening SNIa with a measured $t_2$.

| SN | $L_{max}$ | $e_L$ | $M_{Ni}-Arn$ | $M_{Ni}-DDC$ |
|---|---|---|---|---|
| SN2008gp | 1.29 | 0.14 | | |
| SN2007as | 0.81 | 0.05 | | |
| SN2008bc | 1.32 | 0.19 | | |
| SN2008hv | 1.08 | 0.13 | | |
| SN2008ia | 1.13 | 0.14 | | |
| SN2005na | 1.42 | 0.24 | | |
| SN2005eq | 1.32 | 0.2 | | |
| SN2005M | 1.37 | 0.08 | | |
| SN2007on | 0.6 | 0.09 | | |
| SN2007nq | 0.91 | 0.17 | | |
| SN2005am | 1.1 | 0.2 | | |
| SN2005hc | 1.46 | 0.2 | | |
| SN2004gu | 1.30 | 0.15 | | |
| SN2011fe | 1.1 | 0.15 | | |
| SN2001ba | 1.18 | 0.15 | | |
| SN2002dj | 1.25 | 0.26 | | |
| SN2002fk | 1.42 | 0.23 | | |
| SN2008R | 0.53 | 0.1 | | |
| SN2005iq | 1.07 | 0.11 | | |
| SN2005ki | 1.03 | 0.27 | | |
| SN2006bh | 0.86 | 0.15 | | |
| SN2007bd | 1.22 | 0.13 | | |

Table 3 Coefficients of the best fit relation between $L_{max}$ and $t_2$ in the $YJH$ filters. $a_i$ is the slope in the given filter and $b_i$ is the intercept

| Filter | $a_i$ | $b_i$ |
|---|---|---|
| Y | 0.040 (0.005) | -0.055(0.125) |
| J | 0.042(0.004) | -0.039(0.102) |
| H | 0.033(0.009) | -0.239(0.203) |

### *4.2. Low Galactic Reddening objects*

In our sample, we selected objects with a host galaxy extinction $< 0.1$ mag. For some of these objects, the galactic extinction is $> 0.1$ mag. In order to see whether these objects influence the strength of the correlation, we evaluate the correlation coefficients for a sample without the high galactic reddening objects. As a result, 7 objects with $E(B-V)_{host}$ <0.1 but total E(B-V) $\geq$ are removed. We do not find a substantial decrease in the correlation coefficients in the $YJH$ bands, which are 0.76, 0.83, 0.60 respectively.

Since the reddening law for the MW is known with high certainty, we can correct the bolometric light curves for the absorption from the MW dust. Thus, for further analysis we do not truncate the sample from the original low reddening objects in Table 1

Equations (**??**) relate the timing of the second maximum to the peak bolometric luminosity by combining equation (3) with

equation (**??**). We can see that the relation is dependent on the rise time of the SN and the $\alpha$ parameter which encodes the deviation from Arnett's rule.

From the equations it is evident that the timing of the second maximum in $H$ doesn't provide stringent constraints on the bolometric peak luminosity.

### *4.3. Deriving $M_{Ni}$ from $L_{max}$*

In the sections above, we have found a strong correlation between the peak bolometric luminosity ($L_{max}$) and $t_2$ in the $Y$ and $J$ bands.

Since our final aim is to derive a value of the Nickel mass for objects which have a measured value of $t_2$, we present the different methods to derive $M_{Ni}$ from the peak bolometric luminosity.

#### 4.3.1. Arnett's rule with a variable rise time

Arnett's rule states that the luminosity of the SN at peak is given by the instantaneous rate of energy deposition from radioactive decays inside the expanding ejecta. This is summarized in equation (**??**).

$$L_{max} = \alpha E_{Ni}(t_R) \tag{2}$$

Where $E_{Ni}$ is the input from $^{56}$Ni decay at maximum, $t_R$ is the rise time and $\alpha$ accounts for deviations from Arnett's Rule.

$$E_{Ni}(1M_\odot) = 6.45X10^{43}e^{-t_R/8.8} + 1.45X10^{43}e^{-t_R/111.3} \tag{3}$$

For estimates using different rise times, we follow the relation in **?**

$$t_{R,B} = 17.5 + 5(\Delta m_{15} - 1.1) \tag{4}$$

and

$$t_{R,Bol} = t_{R,B} + (t_{max,bol} - t_{max,B}) \tag{5}$$

which implies

$$L_{max} = \alpha*(6.45X10^{43}e^{-((17.5+5(\Delta m_{15}-1.1)+t_{max,bol}-t_{max,B}))/8.8} 1.45X10^{43}e^{-(17.5+5(\Delta m_{15}-1.1)+t_{max,bol}-t_{max,B}))/111.3})*(M_{Ni}/M_\odot) \tag{6}$$

Since we know that $\Delta m_{15}$ is related to $t_2$, we can rewrite the above equation, in a more compact form as

$$L_{max} = \alpha E_{Ni}(t_2(i)) \tag{7}$$

substituting the relation derived between $L_{max}$ and $t_2$ we get a relation between $t_2$ and $M_{Ni}$

$$(M_{Ni}/M_\odot) = \frac{a_i + t_2(i) + b_i}{\alpha \cdot E_{Ni}(t_2(i))} \tag{8}$$

Equation (8) shows that there is a non-linear relation between $M_{Ni}$ and $t_2(i)$

#### 4.3.2. Arnett's rule with a fixed rise time

For this method of deriving $M_{Ni}$ from $L_{max}$, we use a fixed rise time of 19 days, as in **?**. Similar to their analysis, we propagate an uncertainty of $\pm$ 3 days

$$L_{max} = (2.0 \pm 0.3)X10^{43}(M_{Ni}/M_\odot)ergs^{-1} \tag{9}$$

For deriving equation (9), we use $\alpha$=1.

#### 4.3.3. Interpolating using DDC models

From these bolometric light curves, we derive $M_{Ni}$ values by interpolating the relation between $L_{bol}(max)$ and $M_{Ni}$ from the DDC models of **?** For objects without NIR coverage near maximum, we interpolate the values for the synthetic pseudo-bolometric light curves calculated only using the UBVRI filters. For SN2004gu and SN2007nq, which only has near maximum coverage in the $BVRI$ filters, we use the model value for only that set of filters.

### *4.4. Test Case for SN2014J and SN2006X*

Using the correlations derived above, we want to estimate the Ni masses of heavily reddened SNae. The first test case is the nearby SN 2014J in M82 with an $E(B-V)_{host}$ of 1.3. Current attempts to use the bolometric light curve depend on the $A_V$ value used and vary by a factor of $\sim$ 2 (0.37 $M_\odot$ if using $A_V$=1.7 mag from **?**, compared to 0.77 using a higher $A_V$ of 2.5 mag from **?**). In our analyses the aim is to estimate the $M_{Ni}$ independent of the extinction.

The proximity of SN2014J, has allowed for the first $\gamma$ ray Co line detection in an SNIa (Churazov+ 2014). the authors, using a line photon escape fraction from the models, deduce an Ni mass of 0.62 $\pm$ 0.13 $M_\odot$. This measurement is independent of the $A_V$ value used and is one method of obtaining $M_{Ni}$ for highly reddened objects. However, $\gamma$ ray detections aren't possible for farther away SN, for which we require a different estimation method.

Using the best fit relation for the sample defined above , we obtain $M_{Ni}$ of 0.57 $\pm$ 0.21 $M_\odot$ for a $t_2$ of 28.37 $\pm$ 5.7 days. Thus, we find a very good correspondence between the values from the $\gamma$ rays and the NIR second maximum. This adds evidence to the argument that the NIR can be used for estimate $M_{Ni}$ for highly reddened SN, even in more distant objects for which $\gamma$ ray Co line detections are not possible This uncertainty in $M_{Ni}$ can be reduced with a more precise estimate of $t_2$.

For SN2014J, we can get a precise measurement of the extinction from IR spectra at $\sim$ +300 days. This is again not possible for objects farther away. Thus, we apply this relation to a farther away, heavily extinguished object, SN2006X. The measured value for SN2006X of $t_2(J)$ is 28.19 with an error of 0.63 days. This results in an $M_{Ni}$ value of 0.57 $\pm$ 0.13 $M_\odot$. We can see that a smaller uncertainty in $t_2$ gives a more accurate measurement of $M_{Ni}$. We compare this value for SN2006X to that obtained using $t_2(Y)$ and obtain $M_{Ni}$ of 0.58 $\pm$ 0.17 $M_\odot$. We find both these values consistent with each other. The slightly higher error bar on the value from $t_2(Y)$ is due to a larger error on the intercept in the best fit relation for the $Y$ band. For both SN2014J and SN2006X, the $t_2(H)$ gives an $M_{Ni}$ of 0.50 $\pm$ 0.26 $M_\odot$ and 0.51 $\pm$ 0.23 $M_\odot$ respectively. We can see that a weaker correlation in the $H$ band leads to a slight offset in the $M_{Ni}$ estimate and a larger error bar on the measurement. Hence, we conclude that using the $H$ band to measure the $M_{Ni}$ is not feasible

The derived value of $M_{Ni}$ is consistent with the conclusion that SN2006X is a 'normal' SNIa (**??**).

We include three more objects in the highly reddened sample, namely, 1986G, 2005A and 2008fp. We calculate the $M_{Ni}$ for these objects in the same way as for SN2014J and SN2006X. We summarise our findings in Table 4.4. We can see that 1986G has a lower value of $M_{Ni}$ than the other objects in the sample. This is consistent with the observed optical decline rate and lower $B$ band luminosity of the SN. Since we find that $t_2$ in both

Table 4 $M_{Ni}$ estimates for 5 objects with high values of $E(B-V)_{host}$. We present constraints from the relation using only $t_2(J)$ as well as from both $t_2(Y)$ and $t_2(J)$. We can see a marked decrease in the error values when combined constraints are used

| SN | $M_{Ni}$ (inferred) | $\sigma$ | Method |
|---|---|---|---|
| SN1986G | 0.23 | 0.12 | $J$ band relation |
| – | 0.25 | 0.07 | combined fit |
| SN2005A | 0.54 | 0.15 | $J$ band relation |
| – | 0.56 | 0.07 | combined fit |
| SN2006X | 0.57 | 0.13 | $J$ band relation |
| – | 0.57 | 0.07 | combined fit |
| SN2008fp | 0.63 | 0.15 | $J$ band relation |
| – | 0.65 | 0.07 | cf |
| SN2014J | 0.58 | 0.23 | $J$ band relation |
| – | 0.59 | 0.17 | combined fit |

Table 5 This table summarizes the different methods used to dervie the $M_{Ni}$ values of SN2014J. There is a good agreement between the different methods, however, the bolometric light curves give very different values depending on the reddening assumed-

| $M_{Ni}$ | $e_{M_{Ni}}$ | Method | Reference |
|---|---|---|---|
| 0.62 | 0.13 | $\gamma$ ray $^5 6Co$ line | Churazov 2014 |
| 0.37 | ... | Bolometric lc. $A_V$=1.7 mag | Margutti 2014 |
| 0.77 | ... | Bolometric lc, $A_V$=2.5 | Goobar 2014 |
| 0.58 | 0.17 | $t_2$ combined fit | This work |

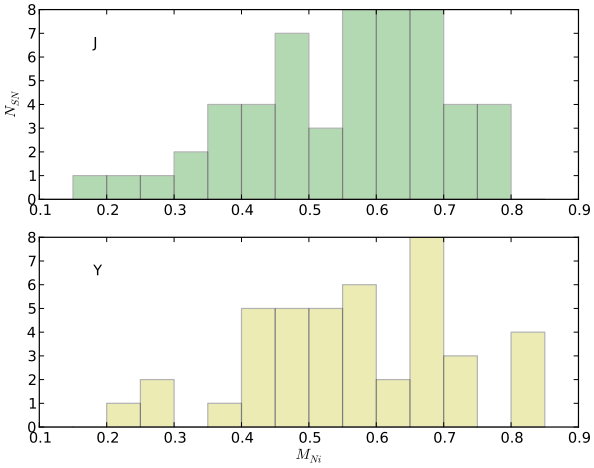


Figure 2 Histogram distributions of $M_{Ni}$ derived from the distributions of $t_2$ for a complete sample of SNIa with measured $t_2$. This uses the Arnett's rule derivation with fixed rise time

$Y$ and $J$ bands correlates very strongly with the $M_{Ni}$, we use combined constraints from the relations to obtain an $M_{Ni}$ estimate. We can see from Table 4.4 that the error on the $M_{Ni}$ reduces when using combined constraints. For 2014J, it is 0.17 $M_\odot$ whereas for the others it is much lower at 0.07 $M_\odot$

Hence, we conclude that the NIR second maximum timing (in $Y$ and $J$) is a very good indicator of the amount of Nickel synthesised in the explosion, even for heavily reddened objects.

### *4.5. Complete NIR Sample*

Since we have derived the relation between $L_{max}$ and $t_2$ and have presented the different ways to obtain the $M_{Ni}$ from the $L_{max}$, we can then use the distribution of $t_2$ for all objects, independent of reddening to obtain a distribution of $M_{Ni}$ using the relations derived

From figure 2, we find a large scatter in the $M_{Ni}$ values. We find that the objects vary by a factor of 3 in their $M_{Ni}$ distribution. We note, however, that since 91bg-like objects do not show a second maximum, we do not have values in the figure $\lesssim 0.2$ $M_\odot$

### *4.6. Comparison with published values*

We searched the literature for published values of $M_{Ni}$ for objects in our sample. In **?** , the authors published values of $M_{Ni}$ for 2005el and 2011fe. For 2011fe, we find $M_{Ni}$ of $0.52 \pm 0.15$ $M_\odot$ whereas the value in S14 is $0.42 \pm 0.08$. We note that the value of $\alpha$ in their study is 1.2 whereas we use $\alpha$=1. Using their value of $\alpha$, we find $M_{Ni}$= 0.44 $M_\odot$, which is a better agreement.

For SN2005el we find $M_{Ni}$ of $0.44 \pm M_\odot$. **?** provides a discussion of this object, which in their sample they measure to have an $M_{Ni}$ of 0.52. It is one of two outliers in their $M_{Ni}$-$\Delta m_{15}$. They argue that it is likely for the SN to have a lower $M_{Ni}$ that their fiducial analysis suggests.

## 5. Discussion and Conclusion

In our sample, we observe a strong correlation between the $M_{Ni}$ and $t_2$ in $Y$ and $J$, and less so in the $H$ band. This provides us with direct evidence that the timing of the second maximum is governed by the amount of Nickel produced by the supernova since it leads to a later ionization transition of the iron group elements at late time (mainly, $^{56}Co$) from doubly to singly ionized (**?**).

This trend is confirmed by a strong correlation between $t_L$ and $M_{Ni}$ indicating that objects with more Ni produced have a slower rate of reddening and the Fe and Co lines appear later in the spectrum, which delays the onset of the lira law phase, and also the second maximum.

This relation offers great insight into measuring the $M_{Ni}$ for objects not in the low-reddening sample, but with extensive NIR data. A striking example of this application is the nearby SN2014J in M82, which is heavily occluded by host galaxy dust. Since this prevents an accurate measurement of $M_{Ni}$ from the bolometric light curves and there is a large disparity in the different values published in the literature using this method, we use the relations we obtain to constrain the $M_{Ni}$. For SN2014J, we have a unique opportunity to compare different estimation methods, since its proximity has allowed $\gamma$ ray Co line detection and therefore, another extinction independent measurement of the $M_{Ni}$. Our value of $0.58 \pm 0.21$ $M_{odot}$ compares very well with **?**, who find $M_{Ni}$ of $0.61 \pm 0.13$ $M_{odot}$. The brightness of SN2014J at late times, due to its proximity, permits us to obtain NIR spectra at $\sim$ 300 days, which can provide an accurate measurement of the extinction and therefore, an accurate $M_{Ni}$ from the bolometric light curve. This presents us with a confrontation of several different methods to measure the $M_{Ni}$ and hence obtain a conclusive estimate on the amount of Ni produce in this SN.

Since $\gamma$ detections are unlikely for farther out SN and most of them are too faint at $\sim$ +300 days for IR spectroscopy, we apply our method to other heavily reddened SN that are farther away than SN2014J. The first object we analyse is SN2006X. From the measurement of $0.57 \pm 0.15$ $M_{odot}$, we conclude that 2006X produced the average amount of Ni for an SNIa.

We also analyse the bolometric light curves at peak and during the late phase of exponential decline. We find that the SN in our sample have a uniform late time bolometric decline rate,

indicating that the internal structure of the ejecta is similar for most SN. This confirms the deductions from the optical and NIR light curves in previous studies and from the bolometric light curves in sample of C00. We also find that the bolometric light curves, unlike the optical light curves, have a narrow distribution of the $\Delta m_{15}$ parameter.

We conclude from our findings that there is a strong dependence of the $t_2$ and the colour evolution (parametrized by $t_L$) on the $M_{Ni}$

## 6. To add

1. $t_l$ versus $M_{Ni}$ plot

2. $M|_{55}$ versus Ni mass in all 3 filters

3. add columns to table 2 with t2 values so that all params are in one set.

4. possibly add ejecta masses too, depending on the point the paper is making

*Acknowledgements.* This research was supported by the DFG cluster of excellence Origin and Structure of the Universe' We would like to thank Chris Burns for his help with template fitting using SNooPy, Richard Scalzo for discussion on the nickel masses and Saraubh Jha on the nature of Type Ia supernovae. We thank Stephane Blondin for his comments on the manuscript. B.L. acknowledges support for this work by the Deutsche Forschungsgemeinschaft through TRR33, The Dark Universe and the Mount Stromlo Observatory for a Distinguished Visitorship during which most of this publication was prepared.